Angle-resolved photoemission spectroscopy study of PrFeAsO_{0.7}: Comparison with LaFePO

I. Nishi, M. Ishikado, S. Ideta, W. Malaeb, T. Yoshida, A. Fujimori, Y. Kotani, M. Kubota, K. Ono, M. Yi, D. H. Lu, R. Moore, Z.-X. Shen, A. Iyo, K. Kihou, H. Kito, H. Eisaki, S. Shamoto, and R. Arita

Phys. Rev. B **84**, 014504 — Published 18 July 2011

DOI: 10.1103/PhysRevB.84.014504

Angle-resolved photoemission spectroscopy study of $PrFeAsO_{0.7}$: Comparison with LaFePO

I. Nishi,[1,*] M. Ishikado,[2,3,4] S. Ideta,[1] W. Malaeb,[1] T. Yoshida,[1,4] A. Fujimori,[1,4] Y. Kotani,[5] M. Kubota,[5] K. Ono,[5] M. Yi,[6] D. H. Lu,[6] R. Moore,[6] Z.-X. Shen,[6] A. Iyo,[3,4] K. Kihou,[3,4] H. Kito,[3,4] H. Eisaki,[3,4] S. Shamoto,[2,4] and R. Arita[7,4,8]

[1]*Department of Physics and Department of Complexity Science and Engineering, University of Tokyo, Hongo, Tokyo 113-0033, Japan*
[2]*Japan Atomic Energy Agency, Tokai, Ibaraki 319-1195, Japan*
[3]*Nanoelectronic Research Institute, National Institute of Advanced Industrial Science and Technology (AIST), Tsukuba, Ibaraki 305-8568, Japan*
[4]*JST, TRIP, Chiyoda, Tokyo 102-0075, Japan*
[5]*Photon Factory, Institute of Materials Structure Science, High Energy Accelerator Research Organization (KEK), Tsukuba, Ibaraki 305-0801, Japan*
[6]*Department of Physics, Applied Physics, and Stanford Synchrotron Radiation Laboratory, Stanford University, Stanford, California 94305, U.S.A.*
[7]*Department of Applied Physics, University of Tokyo, Hongo, Tokyo 113-8656, Japan*
[8]*JST, CREST, Hongo, Tokyo 113-8656, Japan*

We have performed an angle-resolved photoemission spectroscopy (ARPES) study of the iron-based superconductor $PrFeAsO_{0.7}$ and examined the Fermi surfaces and band dispersions near the Fermi level. Heavily hole-doped electronic states have been observed due to the polar nature of the cleaved surfaces. Nevertheless, we have found that the ARPES spectra basically agree with band dispersions calculated in the local density approximation (LDA) if the bandwidth is reduced by a factor of ∼2.5 and then the chemical potential is lowered by ∼70 meV. Comparison with previous ARPES results on LaFePO reveals that the energy positions of the $d_{3z^2-r^2}$- and $d_{yz,zx}$-derived bands are considerably different between the two materials, which we attribute to the different pnictogen height as predicted by the LDA calculation.

PACS numbers: 74.25.Jb, 71.18.+y, 74.70.-b, 79.60.-i
Keywords: pnictides, 1111 system, ARPES

The recent discovery of superconductivity in iron pnictides[1] has attracted keen attention in the materials science community from both experimental and theoretical points of view because they are the only class of superconductors which show critical temperatures (T_c) reaching $\sim$ 56 K[2] other than the cuprates. This new class of iron-based systems share some common properties with the cuprates such as layered crystal structures[1] and antiferromagnetic ordering in the parent compounds[3,4]. However, many differences exist between the two families especially in their electronic structures. These differences started to appear from the early stage when local-density-approximation (LDA) band-structure calculations predicted that many Fe 3*d*-derived bands cross the Fermi level (E_F), resulting in complicated hole- and electron-like Fermi surfaces (FS's)[5–7], whereas only a single band with one FS exists in the cuprates. The predictions of the LDA calculations were confirmed by photoemission experiments, which demonstrated that Fe 3*d* states are predominant near E_F[8–10] with moderate *p*-*d* hybridization and electron correlations[9]. Moreover, angle-resolved photoemission spectroscopy (ARPES) studies have revealed (i) several disconnected hole- and electron-like FS sheets[11], (ii) moderately renormalized energy bands due to electron correlations[12,13], (iii) kinks in the dispersions, suggesting coupling of quasiparticles to boson excitations[14,15], and (iv) FS-dependent nodeless, nearly-isotropic superconducting gaps[16,17,19,20]. Although the mechanism of superconductivity has not been elucidated yet, there is a remarkable correlation between the T_c and the position of pnictogen atoms relative to the Fe plane[21].

The ARPES observations mentioned above were mainly obtained for the so-called 122 system while only a few results have been reported for the 1111 system[13,17,18,22,23] owing to the difficulty in obtaining high quality, sizable single crystals. Because the 1111 system has higher T_c's than those of the 122 system, detailed knowledge of their electronic structure and their differences from that of the 122 system may give a clue for understanding the mechanism of superconductivity in the iron-based superconductors. In the previous ARPES studies on the 1111 system[13,18], heavily hole-doped electronic states have been observed probably due to the polar nature of the cleaved surfaces.

In this work, we have performed ARPES measurements on the 1111 system $PrFeAsO_{0.7}$, which has a T_c as high as $\sim$ 42 K, and compared the results with a band-structure calculation. We have found that the ARPES spectra agree well with the LDA band dispersions and FS's if the calculated bandwidth is reduced by a factor of 2.5 and then the chemical potential is lowered by 70 meV, resulting in heavily hole-doped correlated electronic states. We have thus found remarkable differences in the electronic structures of $PrFeAsO_{0.7}$ and

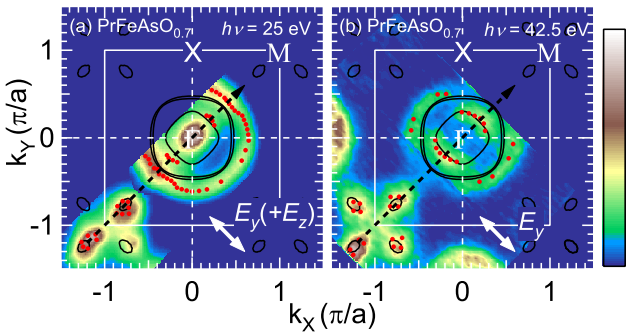

FIG. 1: (Color online) Fermi surface mapping of $PrFeAsO_{0.7}$ obtained by integrating the EDCs over an energy window of $E_F \pm 5$ meV. The white square highlights the boundary of the first Brillouin zone. a is the in-plane lattice constant. The direction of polarization vector is indicated in each panels. Red dots indicate k_F positions determined by the peak positions of momentum distribution curves (MDC's). (a) Fermi surface mapping taken with $h\nu = 25$ eV. (b) Fermi surface mapping taken with $h\nu = 42.5$ eV. Calculated Fermi surfaces (black curves) are plotted on the figures.

LaFePO[13], which can be attributed to the change of the pnictogen height, the distance between the Fe plane and the pnictogen atoms, as predicted by a band structure calculation[30].

High-quality single crystals of the electron-doped compound $PrFeAsO_{0.7}$ ($T_c \sim 42$ K) were synthesized by a high-pressure method described in Ref.[31]. The ARPES measurements were carried out at BL5-4 of Stanford Synchrotron Radiation Laboratory (SSRL), at BL10.0.1 of Advanced Light Source (ALS), and at BL-28A of Photon Factory (PF) using incident photons of $h\nu = 25$ eV linearly-polarized, $h\nu = 42.5$ eV linearly-polarized, and $h\nu =$ 36-80 eV circularly-polarized , respectively. SCIENTA R4000 analyzers were used at SSRL and ALS and a SCIENTA SES-2002 analyzer was used at PF, with a total energy resolution of ∼15 meV and a momentum resolution of $\sim 0.02\ \pi/a$, where $a = 4.0$ Å is the in-plane lattice constant. The crystals were cleaved *in situ* at $T = 10$ K in an ultra-high vacuum better than 1×10^{-10} Torr giving flat mirror-like surfaces which stayed clean all over our measuring time (∼ 2 days). The calibration of E_F of the samples was achieved by referring to that of gold which was in electrical connect with the samples. In the measurements at ALS, the electric field vector of incident photons was in the Fe plane and its direction along the Fe-Fe nearest-neighbor. In the measurements at SSRL, although the direction of the in-plane component of E was the same as that at ALS, E had a component perpendicular to the plane. We have performed a density functional calculation within the LDA by using a WIEN2k package[24], where the experimental tetragonal lattice parameters of PrFeAsO at room temperature were used. As for Pr 4f bands, we have adopted the LSDA+U method in order to remove the bands away from E_F.

Figures 1 (a) and 1(b) show the results of FS mapping for the $PrFeAsO_{0.7}$ sample at low temperature (∼ 10 K) using photon energies $h\nu = 25$ eV and 42.5 eV, respectively. Here, we choose the local coordinate system around the Fe atom such that the x and y axes point toward the nearest-neighbor Fe atoms. The x and y direction are indicated by the electric field vector in Fig 1. In these plots, the photoemission intensity has been integrated over $E_F \pm 5$ meV. In both plots one can clearly observe a large nearly circular hole pocket with $k_F \sim 0.6(\pi/a)$ centered at the Γ point of the the two-dimensional (2D) Brillouin zone (BZ). A smaller nearly circular hole pocket with $k_F \sim 0.3(\pi/a)$ is also seen in Fig. 1 (b) while the intensity is very weak in Fig. 1 (a). In Fig. 1 (b), the momentum regions with strong intensities are opposite between the large and small FS sheets around the Γ point, implying that they have different orbital characters. The large size of the hole pocket has been reported by the previous ARPES studies for the 1111 iron-based superconductors[13,17,18,22] and reflects heavily hole-doped electronic states. One can also observe clover-shaped FS's around the corner (the M point) of the 2D BZ. This occurs because the Fermi level is lowered below the four Dirac points around M caused by excess hole doping. The excess hole doping occurs because the cleaved surface in the 1111 iron pnictides is electronically polar and electronic charges must reconstruct after cleaving[25]. Note that the heavily hole-doped electronic states in the surface region have been observed in spite of the fact the oxygen deficiency of the bulk samples produces negative carrier. The clover-shaped FS's have been also observed in previous ARPES studies of KFe_2As_2[26,27]. We have obtained the same FS's as shown in Figs. 1 (a) and (b) using circularly poralized light (not shown).

The ARPES intensity plots in energy-momentum (E-k) space along the Γ-M direction taken at $h\nu = 25$ eV and 42.5 eV are shown in panels (a) and (b) of Fig. 2, respectively. The direction of the electrical polarization vector of incident light is indicated in Fig. 1. In Fig. 2 (a) and (b), the band dispersions of $PrFeAsO_{0.7}$ deduced from the second derivative plots of EDC's and those of MDC's are also shown (see caption). EDC's of (a) and (b) are shown in panels (e) and (f), respectively. In order to understand the multiband electronic structure of this material, we plot the experimentally deduced band structure and compare with the LDA dispersions for $k_z = 0$ in Fig. 2 (c). We have found that the band structure basically agree with the calculated band dispersions if the bandwidth is reduced by a factor of 2.5 and then the chemical potential is lowered by 70 meV. The band narrowing is due to electron correlations which are not taken into account in our LDA calculation and the chemical potential shift is due to the electronic reconstruction of the surface layers to prevent the "polar catastrophe"[25]. One can also reproduce the observed FS's using the same shift as shown in Figs. 1 (a) and (b). Note that our results reflect surface states and, therefore, k_z dependence

is not expected in the band structures obtained by different photon energies.

According to our LDA calculation [Fig. 2 (c)], the outer two FS's around the Γ point are nearly degenerate and consist of $d_{yz,zx}$ and d_{xy} bands while the inner one consists of only a $d_{yz,zx}$ band. Since the spectral intensity of the d_{xy} band would be weak and may not be seen near the Γ point due to matrix element effects[28], one can conclude that the intensities of both the outer and inner FS's in Figs. 1 (b) and 2 (b) mainly come from the $d_{yz,zx}$ bands. Furthermore, if we take into account matrix element effects for the electric vector E in Fig. 1 (b), the outer and inner FS's have d_{zx} (d_{yz}) and d_{yz} (d_{zx}) orbital character in the k_x (k_y) direction, respectively[35]. However, our band-structure calculation predicts opposite orbital characters between them, namely, d_{yz} (d_{zx}) character for the outer FS and d_{zx} (d_{yz}) character for the inner one along the k_x (k_y) direction[29]. Although the origin of the discrepancy between experiment and our calculation is not clear at present, a similar discrepancy has been reported in a previous ARPES results on a 122 iron-based superconductor[28].

Here, we shall discuss the orbital character of the other bands seen in Figs. 2 (a) and (b). As for the band observed ∼50 meV below E_F around the Γ point, one can notice that the spectral intensity in Fig. 2 (a), where the E_z component is finite, is strong compared to that in Fig. 2 (b). The difference is reliably recognized from Figs. 2 (e) and (f). Therefore, this band is considered to have $d_{3z^2-r^2}$ character as predicted by our band-structure calculation. From Fig. 2 (c), one can also see that the FS around the M point has a hole-like feature arising from the intersection of the $d_{yz,zx}$ band and the d_{xy} band near E_F.

Calculation of the volume enclosed by the hole FS's yields hole counts of 0.07, 0.28 and 0.05 per Fe atom for the inner FS around the Γ point, the outer FS around the Γ point, and the FS's around the M point, respectively. As mentioned above, the spectral intensity of the d_{xy} band should be weak and cannot be observed near the Γ point and, therefore, we cannot evaluate the size of the d_{xy} band FS. For three possible cases, (1) the d_{xy} FS has the same size as the outer FS, (2) it has the same size as the inner FS, and (3) it does not exist, the total hole concentration becomes (1) 0.68, (2) 0.47, and (3) 0.40 holes per Fe atom, respectively. These values are comparable to the predicted value of 0.5 which is necessary to avoid the polar catastrophe[25].

Now, let us compare the present results with the previous ARPES results on LaFePO with T_c ∼6 K[32], which also has the same structure as PrFeAsO with lower pnictogen height than that of $PrFeAsO_{0.7}$. A band structure calculation[30] predicts that if the pnictogen height is lowered, the $d_{3z^2-r^2}$ band is raised and may cross E_F around the Γ point. In order to see differences in the electronic structure between $PrFeAsO_{0.7}$ and LaFePO, in Fig. 2 we compare the present ARPES intensity E-k plot with that of LaFePO[13] along the Γ-M line. For the same reason as mentioned above, $PrFeAsO_{0.7}$ has two bands at the Γ point ∼50 meV and ∼0.2 eV below E_F with $d_{3z^2-r^2}$ character as predicted by the band-structure calculation [Fig. 2 (c)]. In LaFePO, in contrast to $PrFeAsO_{0.7}$, one of the $d_{3z^2-r^2}$ bands crosses E_F and forms a quite large hole FS as shown in Fig. 2 (d). In addition, in LaFePO, the $d_{yz,zx}$ bands around the M point are lowered compared to those in $PrFeAsO_{0.7}$ and recover the electron FS's.

Although we have not been able to observe the spectral intensity of the d_{xy} band near the Γ point as mentioned above, it seems from comparison between the data and our band-structure calculation [Figs. 2 (c) and (d)] that $PrFeAsO_{0.7}$ has a d_{xy} FS around the Γ point while LaFePO does not. According to the theory of spin-flucutuation-mediated superconductibity[33], in which the d_{xy} FS plays an important role to induce high T_c superconductivity, this may be the main reason why the T_c of $PrFeAsO_{0.7}$ is higher than that of LaFePO.

In a previous ARPES study of another 1111 superconductor LaFeAsO[34], the Dirac points around the M point are below E_F like in LaFePO [Fig. 2 (d)], while they are slightly above E_F in $PrFeAsO_{0.7}$ [Fig. 2 (c)]. This difference can also be explained by the change of the different pnictogen heights based on band-structure calculation.

In summary, we have performed an ARPES study of the iron-based superconductor $PrFeAsO_{0.7}$ and revealed the FS's and band dispersions near E_F. Although heavily hole-doped electronic states have been observed, we have found that the ARPES spectra basically agree with the calculated band dispersions if the bandwidth is reduced by a factor of 2.5 and then the chemical potential is lowered by 70 meV. This observation confirms that the LDA calculations for 1111 iron pnictides capture the electronic structure in those compounds. From the comparison of the electronic structures between $PrFeAsO_{0.7}$ and LaFePO, we have demonstrated the pnictogen height dependence of the electronic structure in the 1111 pnictide series as predicted by the band-structure calculations.

The authors acknowledge T. Hanaguri for informative discussions. ALS is operated by the Department of Energy (DOE) Office of Basic Energy Science, Division of Materials Science, under Contract No. DE-AC02-05CH11231. SSRL is operated by the DOE Office of Basic Energy Science Divisions of Chemical Sciences and Material Sciences. Experiment at Photon Factory was approved by the Photon Factory Program Advisory Committee (Proposal No. 2009S2-005). Illuminating discussions at A3 Foresight Program are gratefully acknowledzed. This work was supported by Grant-in-Aid for Scientific Research on Innovative Area "Materials Design through Computics: Complex Correlation and Non-Equilibrium Dynamics" from MEXT.

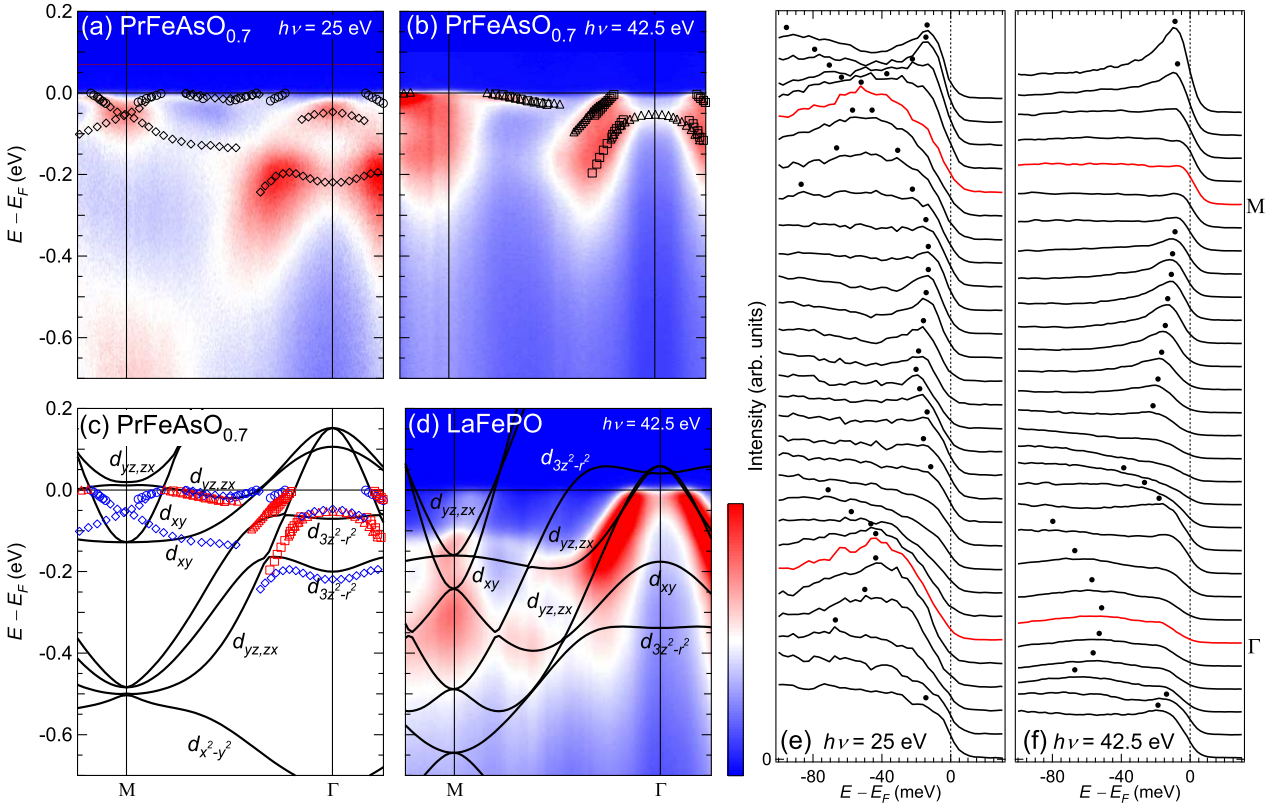

FIG. 2: (Color online) Comparison between ARPES spectra and LDA band structures along the Γ-M direction. The directions of momentum and polarization vector of (a) and (b) are indicated in Fig. 1. (a) The ARPES data taken with $h\nu = 25$ eV. Experimental band structure deduced from the second derivative plots of EDC's and MDC's is also shown. Diamond: EDC peak positions for $h\nu = 25$ eV, circle: MDC peak positions for $h\nu = 25$ eV. (b) The same as (a) with $h\nu = 42.5$ eV. Triangle: EDC peak positions for $h\nu = 42.5$ eV, square: MDC peak positions for $h\nu = 42.5$ eV. (c) Experimental band structure of $PrFeAsO_{0.7}$ deduced from (a) and (b). The calculated band dispersions are plotted after reducing the bandwidth by a factor of 2.5 and then shifting down the chemical potential by 70 meV. (d) The ARPES data of LaFePO taken from Ref.[13]. (e) EDC's obtained from (a). (f) EDC's obtained from (b). Black circles indicate band dispersions.

* Electronic address: nishi@wyvern.phys.s.u-tokyo.ac.jp

[1] Y. Kamihara, T. Watanabe, M. Hirano, and H. Hosono: J. Am. Chem. Soc. **130** (2008) 3296.

[2] C. Wang, L. Li, S. Chi, Z. Zhu, Z. Ren, Y. Li, Y. Wang, X. Lin, Y. Luo, S. Jiang, Z. Xu, G. Cao, and Z. Xu: Europhys. Lett. **83** (2008) 67006.

[3] C. de la Cruz, Q. Huang, J. W. Lynn, J. Li, W. Ratcliff II, J. L. Zarestky, H. A. Mook, G. F. Chen, J. L. Luo, N. L. Wang and P. Dai: Nature **453** (2008) 899.

[4] Q. Huang, Y. Qiu, W. Bao, M. A. Green, J. W. Lynn, Y. C. Gasparovic, T. Wu, G. Wu, and X. H. Chen: Phys. Rev. Lett. **101** (2008) 257003.

[5] K. Kuroki, S. Onari, R. Arita, H. Usui, Y. Tanaka, H. Kontani, and H. Aoki: Phys. Rev. Lett. **101** (2008) 087004.

[6] I.I. Mazin, D.J. Singh, M.D. Johannes and M.H. Du: Phys. Rev. Lett. **101** (2008) 057003.

[7] S. Ishibashi, K. Terakura and H. Hosono: J. Phys. Soc. Jpn. **77** (2008) 053709.

[8] T. Sato, S. Souma, K. Nakayama, K. Terashima, K. Sugawara, T. Takahashi, Y. Kamihara, M. Hirano, and H. Hosono: J. Phys. Soc. Jpn. **77** (2008) 063708.

[9] W. Malaeb, T. Yoshida, T. Kataoka, A. Fujimori, M. Kubota, K. Ono, H. Usui, K. Kuroki, R. Arita, H. Aoki, Y. Kamihara, M. Hirano, and H. Hosono: J. Phys. Soc. Jpn. **77** (2008) 093714.

[10] A. Koitzsch, D. Inosov, J. Fink, M. Knupfer, H. Eschrig, S. V. Borisenko, G. Behr, A. Köhler, J. Werner, B. Büchner, R. Follath, and H. A. Dürr: Phys. Rev. B **78** (2008) 180506(R).

[11] C. Liu, T. Kondo, M. E. Tillman, R. Gordon, G. D. Samolyuk, Y. Lee, C. Martin, J. L. McChesney, S. Bud'ko, M. A. Tanatar, E. Rotenberg, P. C. Canfield, R. Prozorov, B. N. Harmon, and A. Kaminski: Phys. Rev. Lett. **101** (2008) 177005.

[12] L. X. Yang, Y. Zhang, H. W. Ou, J. F. Zhao, D. W. Shen, B. Zhou, J. Wei, F. Chen, M. Xu, C. He, Y. Chen, Z. D. Wang, X. F. Wang, T. Wu, G. Wu, X. H. Chen, M. Arita, K. Shimada, M. Taniguchi, Z. Y. Lu, T. Xiang, and D. L.

Feng: Phys. Rev. Lett. **102** (2009) 107002.
[13] D. H. Lu, M. Yi, S.-K. Mo, A. S. Erickson, J. Analytis, J.-H. Chu, D. J. Singh, Z. Hussain, T. H. Geballe, I. R. Fisher, and Z.-X. Shen: Nature **455**, 81 (2008)
[14] P. Richard, T. Sato, K. Nakayama, S. Souma, T. Takahashi, Y.-M. Xu, G. F. Chen, J. L. Luo, N. L. Wang and H. Ding: Phys. Rev. Lett. **102** (2009) 047003.
[15] L. Wray, D. Qian, D. Hsieh, Y. Xia, L. Li, J. G. Checkelsky, A. Pasupathy, K. K. Gomes, C. V. Parker, A. V. Fedorov, G. F. Chen, J. L. Luo, A. Yazdani, N. P. Ong, N. L. Wang, and M. Z. Hasan: Phys. Rev. B **78** (2008) 184508.
[16] H. Ding, P. Richard, K. Nakayama, K. Sugawara, T. Arakane, Y. Sekiba, A. Takayama, S. Souma, T. Sato, T. Takahashi, Z.Wang, X. Dai, Z. Fang, G. F. Chen, J. L. Luo, and N. L.Wang: Europhys. Lett. **83** (2008) 47001.
[17] T. Kondo, A. F. S.-Syro, O. Copie, C. Liu, M. E. Tillman, E. D.Mun, J. Schmalian, S. L. Budfko, M. A. Tanatar, P. C. Canfield, and A. Kaminski: Phys. Rev. Lett. **101**, 147003 (2008)
[18] D. H. Lu, M. Yi, S.-K. Mo, J.G. Analytis, J.-H. Chu, A.S. Erickson, D.J. Singh, Z. Hussain, T.H. Geballe, I.R. Fisher, Z.-X. Shen: Physica C **469** 452 (2009).
[19] K. Terashima, Y. Sekiba, J. H. Bowen, K. Nakayama, T. Kawahara, T. Sato, P. Richard, Y.-M. Xu, L. J. Li, G. H. Cao, Z.-A. Xu, H. Ding, and T. Takahashi: Proc. Natl. Acad. Sci. U.S.A. **106** (2009) 7330.
[20] K. Nakayama, T. Sato, P. Richard, Y.-M. Xu, Y. Sekiba, S. Souma, G. F. Chen, J. L. Luo, N. L.Wang, H. Ding, and T. Takahashi: Europhys. Lett. **85** (2009) 67002.
[21] C.H. Lee, A. Iyo, H. Eisaki, H. Kito, M. T. Fernandez-Diaz, T. Ito, K. Kihou, H. Mtsuhata, M. Braden, and K. Yamada: J. Phys. Soc. Jpn. **77** (2008) 083704.
[22] H. Liu, G. F. Chen, W. Zhang, L. Zhao, G. Liu, T.-L. Xia, X. Jia,D. Mu, S. Liu, S. He, Y. Peng, J. He, Z. Chen, X. Dong, J. Zhang, G. Wang, Y. Zhu, Z. Xu, C. Chen and X. J. Zhou: Phys. Rev. Lett. **105** 027001 (2010).
[23] M. G. Holder, A. Jesche, P. Lombardo, R. Hayn, D.V. Vyalikh,1 S. Danzenbächer, K. Kummer, C. Krellner, C. Geibel, Yu. Kucherenko, T. K. Kim, R. Follath, S. L. Molodtsov, and C. Laubschat: Phys. Rev. Lett. **104** (2010) 096402.
[24] P. Blaha, K. Schwarz, G. K. H. Madsen, D. Kvasnicka, and J. Luitz: An Augmented Plane Wave + Local Orbitals Program for Calculationg Crystal Properties, (Technische Universitat Wien, Vienna, 2002) [http://www.wien2k.at].
[25] M. Tsukada and T. Hoshino: J. Phys. Soc. Jpn. **51** (1982) 2562.
[26] T. Sato, K. Nakayama, Y. Sekiba, P. Richard, Y.-M. Xu, S. Souma, T. Takahashi, G.F. Chen, J.L. Luo, N.L. Wang, and H. Ding: Phys. Rev. Lett. **103** (2009) 047002.
[27] T. Yoshida, I.Nishi, A.Fujimori, M.Yi, R.G.Moore, D.-H.Lu, Z.-X.Shen, K.Kihou, P.M. Shirage, H.Kito, C.H.Lee, A.Iyo, H.Eisaki, and H.Harima *et al.*, J. Phys. Chem. Solids **72** (2010) 465.
[28] Y. Zhang, B. Zhou, F. Chen, J. Wei, M. Xu, L. X. Yang, C. Fang, W. F. Tsai, G. H. Cao, Z. A. Xu, M. Arita, H. Hayashi, J. Jiang, H. Iwasawa,C. H. Hong, K. Shimada, H. Namatame, M. Taniguchi, J. P. Hu, and D. L. Feng: arXiv:0904.4022v2.
[29] S. Graser, T. A. Maier, P. J. Hirschfeld, and D. J. Scalapino: New J. Phys. 11, 025016 (2009)
[30] V. Vildosola, L. Pourovskii, R. Arita, S. Biermann, and A. Georges: Phys. Rev. B **78** (2008) 064518.
[31] M. Ishikado, S. Shamoto, H. Kito, A. Iyo, H. Eisaki, T. Ito, and Y. Tomioka: Physica C **469** (2009) 901.
[32] Y. Kamihara *et al.*, J. Am. Chem. Soc. **128** (2006) 10012.
[33] K. Kuroki, H. Usui, S. Onari, R. Arita, and H. Aoki: Phys. Rev B **79** (2009) 224511.
[34] L. X. Yang, B. P. Xie, Y. Zhang, C. He, Q. Q. Ge, X. F. Wang, X. H. Chen, M. Arita, J. Jiang, K. Shimada, M. Taniguchi, I. Vobornik, G. Rossi, J. P. Hu, D. H. Lu, Z. X. Shen, Z. Y. Lu, and D. L. Feng: Phys. Rev. B **82** (2010) 104519.
[35] The data of Figs. 1 (b), 2 (b), and 2 (b) have been taken with σ geometry[28]. Therefore, the spectral intensity of d_{zx} band cannot be observed.